

## MIT Open Access Articles

### *Co-expression of CCT subunits hints at TRiC assembly*

The MIT Faculty has made this article openly available. **Please share** how this access benefits you. Your story matters.

**As Published:** <https://doi.org/10.1007/s12192-019-01028-5>

**Publisher:** Springer Netherlands

**Persistent URL:** <https://hdl.handle.net/1721.1/131795>

**Version:** Author's final manuscript: final author's manuscript post peer review, without publisher's formatting or copy editing

**Terms of Use:** Article is made available in accordance with the publisher's policy and may be subject to US copyright law. Please refer to the publisher's site for terms of use.



## Co-expression of CCT Subunits Hints at TRiC Assembly

**Cite this article as:** Oksana A. Sergeeva, Cameron Haase-Pettingell, Jonathan A. King, Co-expression of CCT Subunits Hints at TRiC Assembly, *Cell Stress and Chaperones*, doi: [10.1007/s12192-019-01028-5](https://doi.org/10.1007/s12192-019-01028-5)

This Author Accepted Manuscript is a PDF file of a an unedited peer-reviewed manuscript that has been accepted for publication but has not been copyedited or corrected. The official version of record that is published in the journal is kept up to date and so may therefore differ from this version.

Terms of use and reuse: academic research for non-commercial purposes, see here for full terms. <http://www.springer.com/gb/open-access/authors-rights/aam-terms-v1>

Author accepted manuscript

Co-expression of CCT Subunits Hints at TRiC Assembly

Oksana A. Sergeeva<sup>1,\*</sup>, Cameron Haase-Pettingell<sup>2</sup>, Jonathan A. King<sup>3</sup>

Department of Biology

Massachusetts Institute of Technology

77 Massachusetts Ave. 68-330

Cambridge, MA 02139, USA

1. ORCID: 0000-0002-4830-0518; current address: Global Health Institute, School of Life Sciences, EPFL, Lausanne, Switzerland
2. current address: Computer Science and Artificial Intelligence (CSAIL), Massachusetts Institute of Technology, Cambridge, MA [chaase@mit.edu](mailto:chaase@mit.edu)
3. [jaking@mit.edu](mailto:jaking@mit.edu)

\*corresponding author: [oksana.sergeeva@epfl.ch](mailto:oksana.sergeeva@epfl.ch)

**Abstract**

The eukaryotic cytosolic chaperonin, TCP-1 Ring Complex or TRiC, is responsible for folding a tenth of the proteins in the cell. TRiC is a double-ringed barrel with each ring composed of eight different CCT (Chaperonin Containing TCP-1) subunits. In order for the subunits to assemble together into mature TRiC, which is believed to contain one and only one of each of these subunits per ring, they must be translated from different chromosomes, correctly folded and assembled. When expressed alone in *E. coli*, the subunits CCT4 and CCT5 interestingly form TRiC-like homo-oligomeric rings. To explore potential subunit-subunit interactions, we co-expressed these homo-oligomerizing CCT4 and CCT5 subunits with CCT1-8, or the archaeal chaperonin Mm-Cpn (*Methanococcus mauripaludis* Chaperonin), one at a time. We found that CCT5 shifted all of the CCT subunits, with the exception of CCT6, into double-barrel TRiC-like complexes, while CCT4 only interacted with CCT5 and CCT8 to form chaperonin rings. We hypothesize that these specific interactions may be due to the formation of hetero-oligomers in *E. coli*, although more work is needed for validation. We also observed the interaction of CCT5 and Mm-Cpn with smaller fragments of the CCT subunits, confirming their intrinsic chaperone activity. Based on this hetero-oligomer data, we propose that TRiC assembly relies on subunit exchange with some stable homo-oligomers, possibly CCT5, as base assembly units. Eventually, analysis of CCT arrangement in various tissues and at different developmental times is anticipated to provide additional insight on TRiC assembly and CCT subunit composition.

**Keywords**

Chaperonin, TRiC, CCT, assembly, hetero-oligomer

## Introduction

The eukaryotic chaperonin TRiC is made up of eight different subunits, designated CCT1-CCT8. These subunits are expressed from eight different chromosomes, with CCT6 having two isoforms on two different chromosomes. CCT6A is ubiquitously expressed while CCT6B is more specifically expressed in testes (Kubota et al. 1997). In this manuscript, “CCT” is used for the individual subunits while “TRiC” is used for the full, mature, hetero-oligomeric complex and “micro-complex” is used for CCT oligomers smaller than full TRiC. Expression data of CCTs indicate that all subunits have about equal mRNA quantity, but these amounts as a whole vary between different tissues (Kubota et al. 1999; Yokota et al. 2001a; Boudiaf-Benmammar et al. 2013). At the protein level, there is abundant evidence of the equal stoichiometry of the CCT subunits in TRiC (Rommelaere et al. 1993; Finka and Goloubinoff 2013; Hein et al. 2015).

While it has long been accepted that mature TRiC is made up of two rings of eight different subunits (Liou and Willison 1997; Llorca et al. 2000; Martín-Benito et al. 2007; Cong et al. 2010; Dekker et al. 2011), consensus in the field has been recently reached that the actual arrangement of CCT subunits in TRiC is CCT1-4-2-5-7-8-6-3 with CCT2 and CCT6 making homotypic contacts between the two rings (Kalisman et al. 2012; Leitner et al. 2012). However, earlier studies showed evidence of some CCT subunits being overrepresented in TRiC-like complexes in specific cells, during differentiation, or cell cycle progression (Roobol et al. 1995, 1999b; Yokota et al. 2001b). Technical issues such as epitope promiscuity or steric hindrance could have partly led to these observations. However, it could also be possible that there is a small transient population of immature TRiC-like complexes that contain only a subset of the CCT subunits, for example, to fold large amounts of particular substrates in specific tissues or in early stages of development.

How TRiC actually assembles into the mature complex within a eukaryotic cell has rarely been investigated or addressed in the literature. Almost 20 years ago, it was shown that newly synthesized CCT subunits can assemble onto disassociated single TRiC/CCT rings that would act as thermodynamically favorable templates (Liou et al. 1998). CCT subunits dissociating from TRiC were shown to be in monomers or micro-complexes (Liou et al. 1998). Recently, it was reported that two of the CCT subunits (CCT4 and CCT5) form TRiC-like homo-oligomers when purified from *E. coli* (Sergeeva et

al. 2013). These CCT5 homo-oligomers were crystalized and shown to be similar to TRiC in structure (Pereira et al. 2017). While single monomeric CCT subunits are reported to exist and have roles in eukaryotic cells (Roobol and Carden 1999; Roobol et al. 1999a; Elliott et al. 2015; Spiess et al. 2015), they readily associate with other proteins. This may occur because they are acting as chaperones or because as lone monomers, they are more prone to proteolysis and degradation (Reissmann et al. 2007). Small heat shock chaperones, such as  $\alpha$ -crystallin, can form homo-oligomers but tend to exist as hetero-oligomers by subunit exchange (Bukach et al. 2009; Skouri-Panet et al. 2012). Therefore, we sought to test whether homo-oligomers of CCT4 or CCT5 could incorporate other CCT subunits as a potential first step of TRiC assembly.

To explore TRiC assembly, specifically starting from homo-oligomers of CCT4 or CCT5 and exchanging in the other CCT subunits, we expressed each CCT subunit one at a time, either alone or with CCT4, or with CCT5. Our aim was to investigate whether some CCT subunits were more likely than others to hetero-oligomerize with CCT4 or CCT5 homo-oligomers, suggesting a potential pathway to assembling mature TRiC. Evolution from homo-oligomeric chaperonins such as the ones in *Archaea* to the fully hetero-oligomeric ones in mammals involved gene duplication and positive selection most likely for substrate recognition (Archibald et al. 1999; Horwich et al. 2007; Dekker et al. 2011; Yébenes et al. 2011). Therefore, we also included co-expression with the archaeal chaperonin subunit of *Methanococcus maripaludis* (Mm-Cpn), which forms homo-oligomeric 16-subunit chaperonins endogenously and when expressed in *E. coli* (Reissmann et al. 2007; Knee et al. 2011; Douglas et al. 2011). The domain of the chaperonin that makes the subunit-subunit contacts (equatorial) is well conserved between the CCT subunits and Mm-Cpn so we expected that the ancestral Mm-Cpn would be able to hetero-oligomerize with all CCT subunits. Interestingly, we found that CCT5 hetero-oligomerized with all CCT subunits but CCT6, while CCT4 only hetero-oligomerized with CCT8. Although Mm-Cpn hetero-oligomerized with only four of the CCT subunits, we did find that Mm-Cpn was the most effective at chaperoning CCT fragments. We use this hetero-oligomeric complex formation data to suggest a way of forming the mature hetero-oligomeric TRiC.

## Materials and Methods

*Plasmid Construction*- Two chaperonin subunits at a time were inserted in the pETDuet plasmid (Novagen). The CCT subunit genes (1-8) contained a C-terminal TEV protease cleavage site and a 6x-His-tag, whereas the Mm-Cpn gene was inserted unmodified. Multiple cloning site two (MCS2) contained CCT4, CCT5, Mm-Cpn or nothing, while MCS1 contained CCT1-8, for a total of 32 plasmids. The restriction enzymes for CCT1-8 in MCS1 were SpeI and AscI, where SpeI was inserted into the plasmid via mutagenesis. For MCS2, the restriction enzymes for CCT4 and CCT5 were NdeI and KpnI, while for Mm-Cpn they were NdeI and BamHI. All (32 in total) plasmids were confirmed by sequencing (Genewiz).

*Expression and lysis*- Plasmids were transformed into *E. coli* BL21 (DE3) RIL cells (Agilent). Cells were grown in Super Broth to OD 5.0 at 37 °C and then shifted to 18 °C and induced with 0.5 mM IPTG. After the overnight induction, cultures were pelleted by centrifugation for 15 min, and the cells were resuspended in CCT-A Buffer (20 mM HEPES/KOH pH 7.4, 300 mM NaCl, 10 mM MgCl<sub>2</sub>, 10% glycerol, 1 mM DTT, 1 mM ATP) with addition of one EDTA-free complete protease inhibitor (Roche) per L of culture. To lyse the cells, 1 mM DTT, 5 mM MgCl<sub>2</sub>, and 2.5 mg/mL lysozyme, and 10 µg/mL DNase were added to the pellets. After an incubation with shaking at approximately 12 °C, the cells were lysed via French Press. Debris was spun down at 11,500 x g and supernatant was isolated by pipetting.µ

*Sucrose gradient sedimentation*- Using CCT-A buffer, 5-40% sucrose gradients were prepared using the gradient master (BioComp Instruments). Lysates (100 µL) were added carefully to the top and gradients were ultracentrifuged at 4 °C for 18 h at 28,000 rpm using a SW50 rotor (Beckman). Nineteen or twenty fractions were collected using a gradient fractionator (BioComp Instruments), and one bottom fraction was collected from the leftover gradient. To disrupt ribosomes, lysates were treated with 50 mM EDTA and 0.2 mg/mL RNase in CCT-A buffer before ultracentrifugation application.

*CCT subunit purification, mass spectrometry, electron microscopy*- CCT1 was purified as described for the CCT subunits (Sergeeva et al. 2013). Briefly, *E. coli* cells were lysed by French Press and debris were pelleted. The supernatant was passed over a nickel-nitrilotriacetic acid (Ni-NTA) column and eluted off using a linear gradient to 250 mM imidazole. Fractions containing CCT1 were combined and incubated with TEV protease to cleave the His-tag and then passed over the Ni-NTA column again. The flow through was collected and separated using size exclusion chromatography. Mass spectrometry was

performed, as described previously (Sergeeva et al. 2013), in the Biopolymer and Proteomic Core Facility at the Koch Institute (Cambridge, MA). Negative-stain electron microscopy (EM) was performed as described earlier (Sergeeva et al. 2013, 2014). Briefly, samples were applied to glow-discharged copper grids, then the grids were floated upside down in 1.5% uranyl acetate for 45 s. Grids were imaged using a JEOL 1200 SX transmission EM with a AMT 16000S camera system.

*SDS-PAGE and immunoblots*- Proteins were separated by SDS-PAGE (10%) at 165 V for 1 h after boiling in reducing buffer (60 mM Tris, pH 6.8, 2% SDS, 5%  $\beta$ -mercaptoethanol, 10% glycerol, bromophenol blue for color) for 5 min. The gels were stained with Coomassie blue or Krypton Fluorescent Protein Stain (ThermoFisher Scientific). Transfer was conducted for 1.5 h at 300 mA in transfer buffer (10% methanol, 25 mM Tris, 192 mM glycine) onto 0.45  $\mu$ m polyvinylidene difluoride (PVDF) membranes (Millipore). The primary antibodies were from Santa Cruz Biotechnology: CCT1, sc-53454; CCT2, sc-28556; CCT3, sc-33145; CCT4, sc-137092; CCT5, sc-13886; CCT6, sc-100958; CCT7, sc-130441; and, CCT8, sc-13891. An anti-His(C-term)-AP antibody (Life technologies) was used for further verification. The secondary antibodies were Alkaline Phosphatase (AP)-conjugated (Millipore) and the membranes were visualized using the AP-conjugate substrate kit (BioRad).

*Quantification*- Band quantification was done using ImageJ for both full-length and fragments of the CCT subunits. The band densities of all 19 fractions (20 for CCT1) were summed and each fraction was divided by the total to calculate a percentage of the total density of the gradient in each fraction. All graphs were created in GraphPad Prism.



## Results

### *Framework and Controls to Study Pair-wise Chaperonin Interactions*

In order to investigate how TRiC is assembled, we utilized the properties of CCT4, CCT5, and the archaeal Mm-Cpn to assemble into homo-oligomers in *E. coli* (Reissmann et al. 2007; Sergeeva et al. 2013). We used the pETDuet plasmid and constructed a repository of 32 plasmids to study pair-wise chaperonin-subunit interactions. The plasmids were expressed in *E. coli* BL21 (DE3) RIL cells. The cells were lysed and applied to sucrose ultracentrifugation gradients, whose fractions were run on SDS-PAGE. Krypton-stained SDS-PAGE profiles of the ultracentrifugation gradients looked similar for all lysates, suggesting that overall *E. coli* proteins were not significantly affected (representative gels for CCT2 shown in Fig. 1). The only notable exception was the higher abundance of Mm-Cpn when it was co-expressed. In order to investigate the human CCT subunits, gels were transferred and immunoblotted against the appropriate CCT subunit corresponding to CCT1-8. These gradients can separate the CCT species into monomers or micro-complexes, TRiC-like complexes, or faster-sedimenting aggregates or ribosome-associated species (Fig. 2A). Both the slowly-sedimenting monomer and micro-complex species and the ribosome-associated faster-sedimenting species were observed previously in mammalian cell lysates, suggesting that these species are physiologically relevant (Frydman et al. 1994; Liou and Willison 1997; Roobol et al. 1999a). For all the CCT subunits, we detected a species corresponding to the approximately 60-kDa full-length CCT species (Fig. 2B). Each full-length CCT subunit expressed alone from the pETDuet plasmid had a similar sedimentation pattern as found for that subunit expressed from the pET21a plasmid (Sergeeva et al. 2013).

The co-expression of full-length CCT1-8 in the pETDuet plasmid did not change the expression patterns of CCT4, CCT5, or Mm-Cpn as seen by immunoblotting against CCT4 or CCT5 when another CCT was expressed (Fig. 3). While CCT4, CCT5, and Mm-Cpn complexes sediment slightly differently in the gradients (shown previously (Sergeeva et al. 2014)), in this study, we use the term “complex” to designate the sedimentation of TRiC-like complexes to encompass all three homo-oligomer complex species. Considering the full-length CCT species, some – CCT1 and CCT2 alone, and, to a lesser degree, CCT6 and CCT8 alone – show unique enrichment in species sedimenting faster than complexes. This is a region of gradients that contains small aggregates or is enriched in ribosomes (Sergeeva et al.

2014). To verify ribosome association, we disrupted the ribosomes with RNase and EDTA (Wedeken et al. 2010; Simsek et al. 2017) and found a decrease in the faster-sedimenting species (Fig. 4A), indicating that the species near the bottom of the gradients were indeed ribosome-associated. We further tried to purify CCT1 the same way we previously purified CCT4 and CCT5 homo-oligomers (Sergeeva et al. 2013), but found that CCT1 purity after three chromatography steps was limited (Fig. 4B). When the purest fraction was viewed by negative-stain EM (Fig. 4C), contaminating ribosomes and GroE were detected. GroE contamination was likely due to the enrichment of complex-sized species, but ribosomes persisting through the purification implied that CCT1 chains are truly associated with ribosomes. Even further, mass spectrometry analysis of the “purified” CCT1 fraction revealed not only mammalian CCT1 but also bacterial chaperones and ribosomal proteins (Fig. 4D). In all, the data support the ribosome association mentioned in previous publications. However, we also observe CCT subunit aggregates in the faster-than-complex sedimenting region.

#### *CCT Homo-oligomers Incorporating Other Full-length CCT Subunits*

The full-length CCT species were quantified to analyze the changes in sedimentation patterns between the CCT subunits alone and their co-expression with homo-oligomerizing CCT4, CCT5, or Mm-Cpn (Fig. 5A). Most relevant for the investigation of CCT interactions on the way to TRiC assembly is the formation of TRiC-like complexes when the CCT subunits are co-expressed with homo-oligomeric subunits. Considering this, all CCT subunits but CCT6 had an enrichment in complex species when co-expressed with CCT5. Mm-Cpn was the second most effective, interacting with CCT2, CCT3, and maybe CCT6, in the complex part of the gradient. CCT4 was least effective, only showing any complex interaction with CCT5 and CCT8. Using the enriched complex species of the gradients, we constructed a binary heat map to show the presence of these interactions (Fig. 5B). We use this interaction data to postulate on the assembly properties and evolutionary background of TRiC.

#### *CCT Homo-oligomers Chaperoning Full-length CCT Subunits and CCT Subunits Fragments*

One of the main functions of chaperonins is to bind and fold other protein chains. Thus, we appropriately observed chaperone properties of the homo-oligomers in our system. However, the extent

and variation of these interactions was remarkable. For the full-length species, the gradients of CCT1, CCT2, CCT6 and CCT8 alone indicate that the faster-sedimenting species are significantly decreased or eliminated in the presence of CCT4, CCT5, or Mm-Cpn (Fig. 5A). This suggests that the homo-oligomerizing chaperonins may interact with these particular CCT subunits to dissociate them from the ribosomes or aggregation. One overarching pattern seen in the gradients was that when co-expressed with Mm-Cpn, all full-length CCT subunits were found to sediment as micro-complexes. It is possible that these species could represent single Mm-Cpn rings that possess chaperone function. When co-expressed with CCT4 or to a lesser extent CCT5, some full-length CCT subunits (CCT1, CCT2, and CCT6) which alone show faster-sedimenting species, are enriched in the monomer species of the gradient. This implies that CCT4 causes these CCT subunits to dissociate into stable smaller species. Thus, as chaperones, CCT4, CCT5, and Mm-Cpn homo-oligomers indeed have a role in binding to, chaperoning, and potentially folding full-length CCT subunits, but more for some (Mm-Cpn) than others (CCT5).

All CCT subunits except CCT6 displayed various fragments (representative blots for CCT1 shown in Fig. 6A). These fragments included mid-length fragments, such as the CCT4 fragment of 53 kDa that has been previously observed and preliminarily characterized (Sergeeva et al. 2013). Many fragments are a result of protease cleavage in the lid of the chaperonin, which results in two approximately equal peptides. Overall, fragment co-expression with CCT4, CCT5, and Mm-Cpn homo-oligomers led to very few pattern changes in the gradients. The most notable enrichments were Mm-Cpn co-expression allowing many fragments to move to complexes while CCT5 co-expression shifting the 30-kDa CCT1 fragment to complexes (Fig. 6B). In addition, CCT5 co-expression enriched two species (45-kDa CCT1 and 42-kDa CCT3) into monomer subunits while CCT4 co-expression enhanced two species (30-kDa and 42-kDa CCT1) into micro-complexes.

The movement of the CCT subunit fragments to complexes or slower-sedimenting regions of the gradient in the presence of co-expressed CCT4, CCT5, or Mm-Cpn suggests that we are indeed observing binding, chaperoning, and maybe folding properties of the homo-oligomerizing chaperonins. This is especially true for Mm-Cpn, which displays this property for many of its interactions (6 of the 12 fragments quantified). Expression of CCT4 and CCT5 homo-oligomers show much less of these

chaperoning properties (2 out of 12 fragments quantified), suggesting that they are less likely to interact with CCT subunit fragments (Fig. 6B).

## Discussion

Our experiments represent a first step toward understanding possible interactions between CCT subunits *en route* to mature hetero-oligomeric TRiC assembly. The most crucial next step is to learn whether these interactions are *bona fide* hetero-oligomeric interactions or whether the homo-oligomers are actually chaperoning the CCT subunits with which they interact. While we cannot achieve that directly using these constructs and methods, we now have collected crucial hints from understanding the interactions of these fragments. Some transient chaperoning function was observed as a few of the full-length CCTs and subunit fragments were found to sediment as either monomers or micro-complexes in the presence of CCT4 or CCT5 homo-oligomers. However, Liou and colleagues reported 20 years ago (Liou et al. 1998) that TRiC was not found to chaperone its own subunits. The discrepancy could lie in the fact that CCT4, CCT5 or especially Mm-Cpn homo-oligomers don't have the same substrate recognition properties as full hetero-oligomeric TRiC or that the CCT subunits studied here may need help folding or assembling from other chaperones in eukaryotic cells. On the other hand, we found that none of CCT fragments were found in the complex region when co-expressed with CCT4 and CCT5 homo-oligomers, suggesting that we are detecting real hetero-oligomeric interactions of full-length CCT species in the complex regions.

Mm-Cpn interacted with nearly all of the full-length CCTs and many of the fragments to shift them either in a micro-complex or complex species. It is likely Mm-Cpn could be trapping these fragments in its cavity as was observed by cryo-EM for CCT5 homo-oligomers. This suggests that Mm-Cpn is primarily chaperoning rather than hetero-oligomerizing, as we had initially postulated. In the example of the V-ATPase, the  $V_0$  ring evolved due to changes in protein interfaces rather than new function (Finnigan et al. 2012). Thus, we had hypothesized that as the ancestral homolog of a complex of paralogs that underwent positive selection in the substrate binding domain (Fares and Wolfe 2003), Mm-Cpn could still retain its ability to associate through its conserved subunit-subunit domain with all of the CCT subunits. Previous studies also have shown that CCT4 and CCT5 are most closely associated to the archaeal chaperonins

(Archibald et al. 2000), possibly corroborating their homo-oligomeric nature. Based on our data, there must have been evolution in the subunit-subunit contacts of the CCT subunits, so much so, that many CCT subunits can no longer hetero-oligomerize with Mm-Cpn. This evolution corroborates the existence of only one specific arrangement of the CCT subunits in mature TRiC (Kalisman et al. 2012; Leitner et al. 2012). Even so, some ancestral structure relationship remains to allow Mm-Cpn to hetero-oligomerize with CCT2 and CCT3.

If our hypothesis that the dual expressed CCTs form CCT hetero-oligomers is correct, we can use our data to better analyze TRiC assembly and structure. CCT6 not interacting with CCT4 nor CCT5 is consistent with the final TRiC structure, as it makes homo-typic contacts between rings and contacts CCT3 and CCT8 within the rings. Our data for CCT4 not interacting with CCT1 nor CCT2 is inconsistent with the final TRiC arrangement wherein CCT4 interacts with these two subunits. However, we did find that CCT4 was able to enrich monomer formation of CCT1 and CCT2, suggesting that they do somehow interact. Furthermore, observing the interaction between CCT4 and CCT8 is surprising from the side of the final TRiC structure. We, therefore, suggest that CCT4 and CCT8 may interact during the assembly of TRiC, or this association is a remaining evolutionarily remnant. Based on previous work, CCT4 is generally less well behaved as a homo-oligomer than CCT5 (Sergeeva et al. 2013, 2014), possibly explaining its fewer interactions. In all, CCT5 homo-oligomers may be more probable starting point. From there, subunit exchange could take place to form the final TRiC structure. **We propose one assembly model based on our data and the final known CCT order (Fig. 7). This model has CCT2 as the first CCT subunit to incorporate in the chaperonin with the others following suit because the interactions between neighboring subunits in the mature complex are more favorable than interactions with CCT5 or others. Based on the data, CCT6, due to its lack of interactions, would assemble last. It is important to note that the stoichiometry of the subunits is still roughly equal *in vivo*, so CCT5 homo-oligomer complexes would be surrounded by 16 molecules of the other CCT subunits. One mystery is what would happen to the single CCT5 subunits once they are replaced. Future research on CCT subunit dynamics will shed light on this thermodynamic conundrum.**

While the above model is hypothetical, emerging experimental methods will be able to detect small amounts of chaperonin with non-mature arrangement, while modeling can be employed to

investigate the likelihood of these models given the strength of subunit-subunit interactions. As mentioned earlier, the CCTs are transcribed from many different chromosomes. This means that the assembly of TRiC in the cell has to be regulated both temporally and spatially. One way to allow the cytosolic CCTs to assemble in the crowded environment of the cell is to target them to a specific subcellular compartment. A recent study showed that all of the CCT subunits are palmitoylated (Blanc et al. 2015), suggesting that the subunits can be attached to the endoplasmic reticulum or plasma membrane, giving them access to each other and the emerging complex in 2D space. Palmitoylation is a reversible modification that can affect a protein in many ways including localization, stability, or function (Chamberlain and Shipston 2015; Zaballa and van der Goot 2018). In the case of TRiC, CCT4 and CCT5 homo-oligomers are stable and functional when purified out of *E.coli* (Sergeeva et al. 2013), suggesting that this modification may only play a role in the assembly of the complex and not its activity.

Future research is needed to clarify exactly how TRiC assembles and what could assist its assembly, especially in specific tissues, during development, or while cells undergo differentiation. One of the best ways to further investigate this is by doing quantitative mass spectrometry of the co-expressed species to understand their complex stoichiometry. **Expression of more than two CCT subunits a time may also give data to support or reject our proposed model. *In vitro* assembly methods with such sensitive readouts have not yet been attempted on this complicated complex.** Even further, *in vitro* mixing of various CCT subunits until they reach equilibrium and exchange into TRiC-like rings would help verify the model. Over 20 years ago, a few years after the discovery of TRiC, Kubota et al. posed eleven most interesting and pressing questions about TRiC in a review (Kubota et al. 1995). Many of them have been addressed or fully answered (substrates, arrangement, ATPase properties, among others) but the topic of TRiC assembly has been generally overlooked. Our work represents a step from which we can dig deeper to answer this question.

### **Acknowledgements**

We would like to thank the members of the Jonathan King lab for helpful discussions on this topic and the members of Gisou van der Goot lab for critical reading of this manuscript.

## References

- Archibald JM, Logsdon JM, Doolittle WF (2000) Origin and evolution of eukaryotic chaperonins: phylogenetic evidence for ancient duplications in CCT genes. *Mol Biol Evol* 17:1456–1466. doi: 10.1093/oxfordjournals.molbev.a026246
- Archibald JM, Logsdon JM Jr, Doolittle WF (1999) Recurrent paralogy in the evolution of archaeal chaperonins. *Curr Biol* 9:1053–1056
- Blanc M, David F, Abrami L, et al (2015) SwissPalm: Protein Palmitoylation database. *F1000Res* 4:261. doi: 10.12688/f1000research.6464.1
- Boudiaf-Benmammar C, Cresteil T, Melki R (2013) The Cytosolic Chaperonin CCT/TRiC and Cancer Cell Proliferation. *PLoS ONE* 8:e60895. doi: 10.1371/journal.pone.0060895
- Bukach OV, Glukhova AE, Seit-Nebi AS, Gusev NB (2009) Heterooligomeric complexes formed by human small heat shock proteins HspB1 (Hsp27) and HspB6 (Hsp20). *Biochimica et biophysica acta* 1794:486–95. doi: 10.1016/j.bbapap.2008.11.010
- Chamberlain LH, Shipston MJ (2015) The physiology of protein S-acylation. *Physiol Rev* 95:341–376. doi: 10.1152/physrev.00032.2014
- Cong Y, Baker ML, Jakana J, et al (2010) 4.0-Å resolution cryo-EM structure of the mammalian chaperonin TRiC/CCT reveals its unique subunit arrangement. *Proc Natl Acad Sci* 107:4967–4972. doi: 10.1073/pnas.0913774107
- Dekker C, Roe SM, McCormack EA, et al (2011) The crystal structure of yeast CCT reveals intrinsic asymmetry of eukaryotic cytosolic chaperonins. *EMBO J* 30:3078–3090. doi: 10.1038/emboj.2011.208
- Douglas NR, Reissmann S, Zhang J, et al (2011) Dual Action of ATP Hydrolysis Couples Lid Closure to Substrate Release into the Group II Chaperonin Chamber. *Cell* 144:240–252. doi: 10.1016/j.cell.2010.12.017
- Elliott KL, Svanstrom A, Spiess M, et al (2015) A novel function of the monomeric CCTepsilon subunit connects the serum response factor pathway to chaperone-mediated actin folding. *Molecular biology of the cell* 26:2801–9. doi: 10.1091/mbc.E15-01-0048
- Fares MA, Wolfe KH (2003) Positive Selection and Subfunctionalization of Duplicated CCT Chaperonin Subunits. *Mol Biol Evol* 20:1588–1597. doi: 10.1093/molbev/msg160
- Finka A, Goloubinoff P (2013) Proteomic data from human cell cultures refine mechanisms of chaperone-mediated protein homeostasis. *Cell Stress Chaperones* 18:591–605. doi: 10.1007/s12192-013-0413-3
- Finnigan GC, Hanson-Smith V, Stevens TH, Thornton JW (2012) Evolution of increased complexity in a molecular machine. *Nature* 481:360–364. doi: 10.1038/nature10724
- Frydman J, Nimmegern E, Ohtsuka K, Hartl FU (1994) Folding of nascent polypeptide chains in a high molecular mass assembly with molecular chaperones. *Nature* 370:111–117. doi: 10.1038/370111a0
- Hein MY, Hubner NC, Poser I, et al (2015) A Human Interactome in Three Quantitative Dimensions Organized by Stoichiometries and Abundances. *Cell* 163:712–723. doi: 10.1016/j.cell.2015.09.053

- Horwich AL, Fenton WA, Chapman E, Farr GW (2007) Two Families of Chaperonin: Physiology and Mechanism. *Annu Rev Cell Dev Biol* 23:115–145. doi: 10.1146/annurev.cellbio.23.090506.123555
- Kalisman N, Adams CM, Levitt M (2012) Subunit order of eukaryotic TRiC/CCT chaperonin by cross-linking, mass spectrometry, and combinatorial homology modeling. *Proc Natl Acad Sci* 109:2884–2889. doi: 10.1073/pnas.1119472109
- Knee KM, Goulet DR, Zhang J, et al (2011) The group II chaperonin Mm-Cpn binds and refolds human  $\gamma$ D crystallin. *Protein Sci* 20:30–41. doi: 10.1002/pro.531
- Kubota H, Hynes G, Willison K (1995) The chaperonin containing t-complex polypeptide 1 (TCP-1). *Eur J Biochem* 230:3–16
- Kubota H, Hynes GM, Kerr SM, Willison KR (1997) Tissue-specific subunit of the mouse cytosolic chaperonin-containing TCP-1. *FEBS Lett* 402:53–56
- Kubota H, Yokota S, Yanagi H, Yura T (1999) Structures and co-regulated expression of the genes encoding mouse cytosolic chaperonin CCT subunits. *Eur J Biochem* 262:492–500
- Leitner A, Joachimiak LA, Bracher A, et al (2012) The Molecular Architecture of the Eukaryotic Chaperonin TRiC/CCT. *Struct* 20:814–825. doi: 10.1016/j.str.2012.03.007
- Liou AK, McCormack EA, Willison KR (1998) The chaperonin containing TCP-1 (CCT) displays a single-ring mediated disassembly and reassembly cycle. *Biol Chem* 379:311–319
- Liou AKF, Willison KR (1997) Elucidation of the subunit orientation in CCT (chaperonin containing TCP1) from the subunit composition of CCT micro-complexes. *EMBO J* 16:4311–4316
- Llorca O, Martín-Benito J, Ritco-Vonsovici M, et al (2000) Eukaryotic chaperonin CCT stabilizes actin and tubulin folding intermediates in open quasi-native conformations. *EMBO J* 19:5971–5979. doi: 10.1093/emboj/19.22.5971
- Martín-Benito J, Grantham J, Boskovic J, et al (2007) The inter-ring arrangement of the cytosolic chaperonin CCT. *EMBO Rep* 8:252–257. doi: 10.1038/sj.embor.7400894
- Pereira JH, McAndrew RP, Sergeeva OA, et al (2017) Structure of the human TRiC/CCT Subunit 5 associated with hereditary sensory neuropathy. *Scientific Reports* 7:3673. doi: 10.1038/s41598-017-03825-3
- Reissmann S, Parnot C, Booth CR, et al (2007) Essential function of the built-in lid in the allosteric regulation of eukaryotic and archaeal chaperonins. *Nat Struct Mol Biol* 14:432–440. doi: 10.1038/nsmb1236
- Rommelaere H, Van Troys M, Gao Y, et al (1993) Eukaryotic cytosolic chaperonin contains t-complex polypeptide 1 and seven related subunits. *Proc Natl Acad Sci* 90:11975–11979
- Roobol A, Carden MJ (1999) Subunits of the eukaryotic cytosolic chaperonin CCT do not always behave as components of a uniform hetero-oligomeric particle. *Eur J Cell Biol* 78:21–32
- Roobol A, Grantham J, Whitaker HC, Carden MJ (1999a) Disassembly of the cytosolic chaperonin in mammalian cell extracts at intracellular levels of K<sup>+</sup> and ATP. *J Biol Chem* 274:19220–19227
- Roobol A, Holmes FE, Hayes NVL, et al (1995) Cytoplasmic chaperonin complexes enter neurites developing in vitro and differ in subunit composition within single cells. *J Cell Sci* 108:1477–1488



- Roobol A, Sahyoun ZP, Carden MJ (1999b) Selected subunits of the cytosolic chaperonin associate with microtubules assembled in vitro. *J Biol Chem* 274:2408–2415
- Sergeeva OA, Chen B, Haase-Pettingell C, et al (2013) Human CCT4 And CCT5 Chaperonin Subunits Expressed in Escherichia coli Form Biologically Active Homo-oligomers. *J Biol Chem* 288:17734–17744. doi: 10.1074/jbc.M112.443929
- Sergeeva OA, Tran MT, Haase-Pettingell C, King JA (2014) Biochemical characterization of mutants in chaperonin proteins CCT4 and CCT5 associated with hereditary sensory neuropathy. *The Journal of biological chemistry* 289:27470–80. doi: 10.1074/jbc.M114.576033
- Simsek D, Tiu GC, Flynn RA, et al (2017) The mammalian ribo-interactome reveals ribosome functional diversity and heterogeneity. *Cell* 169:1051-1065.e18. doi: 10.1016/j.cell.2017.05.022
- Skouri-Panet F, Michiel M, Ferard C, et al (2012) Structural and functional specificity of small heat shock protein HspB1 and HspB4, two cellular partners of HspB5: role of the in vitro hetero-complex formation in chaperone activity. *Biochimie* 94:975–84. doi: 10.1016/j.biochi.2011.12.018
- Spiess M, Echbarthi M, Svanstrom A, et al (2015) Over-Expression Analysis of All Eight Subunits of the Molecular Chaperone CCT in Mammalian Cells Reveals a Novel Function for CCTdelta. *Journal of molecular biology* 427:2757–64. doi: 10.1016/j.jmb.2015.06.007
- Wedeken L, Ohnheiser J, Hirschi B, et al (2010) Association of Tumor Suppressor Protein Pcd4 With Ribosomes Is Mediated by Protein-Protein and Protein-RNA Interactions. *Genes & Cancer* 1:293–301. doi: 10.1177/1947601910364227
- Yébenes H, Mesa P, Muñoz IG, et al (2011) Chaperonins: two rings for folding. *Trends Biochem Sci* 36:424–432. doi: 10.1016/j.tibs.2011.05.003
- Yokota S, Yamamoto Y, Shimizu K, et al (2001a) Increased expression of cytosolic chaperonin CCT in human hepatocellular and colonic carcinoma. *Cell Stress Chaperones* 6:345–350
- Yokota S, Yanagi H, Yura T, Kubota H (2001b) Cytosolic chaperonin-containing t-complex polypeptide 1 changes the content of a particular subunit species concomitant with substrate binding and folding activities during the cell cycle. *European Journal of Biochemistry* 268:4664–4673. doi: 10.1046/j.1432-1327.2001.02393.x
- Zaballa M-E, van der Goot FG (2018) The molecular era of protein S-acylation: spotlight on structure, mechanisms, and dynamics. *Critical Reviews in Biochemistry and Molecular Biology* 53:420–451. doi: 10.1080/10409238.2018.1488804

## Figure Legends

**Figure 1.** *Krypton-stained SDS-PAGE sucrose gradient ultracentrifugation of CCT2 co-expressed in E.coli alone, with CCT4, CCT5, or Mm-Cpn.* Lysed cells expressing pETDuet plasmids with CCT2 subunit alone, with CCT4, with CCT5, or with Mm-Cpn were applied to sucrose gradients and then fractionated. The fractions were run on 10% SDS-PAGE and stained with Krypton fluorescent protein stain (top, 5% to 40%, bottom). Fractions are separated by dotted vertical lines for easier visual comparison and fractions corresponding to approximately the complex region of the gradient are outlined in vertical lines. The 60-kDa species seen between the two solid lines in the middle of the gradient for CCT2 alone is GroEL. Co-expressions of CCT5 and Mm-Cpn have a more pronounced species there as it is the overexpression of CCT5 and Mm-Cpn themselves. Representative gels are shown for CCT2 but other CCT subunits are similar at the Krypton-stained SDS-PAGE level. Colors for CCT4 (4; orange), CCT5 (5; green), and Mm-Cpn (M; blue) correspond to the colors shown in the other figures.

**Figure 2.** *A. Chaperonin species present in a sucrose sedimentation gradient.* Species of chaperonin (Mm-Cpn shown in this case – PDB: 3K01, 3KFB – with its domains colored differently) are depicted at their sedimentation positions. *B. Immunoblot SDS-PAGE of sucrose gradient ultracentrifugation of full-length CCT1-CCT8 co-expressed in E.coli alone, with CCT4, CCT5, or Mm-Cpn.* Lysed cells expressing pETDuet plasmids with each CCT subunit alone, with CCT4, with CCT5, or with Mm-Cpn were applied to sucrose gradients and then fractionated. The fractions were run on 10% SDS-PAGE, transferred, probed with the corresponding CCT antibody, and shown here (top, 5% to 40%, bottom). Fractions corresponding to approximately the complex region of the gradient are outlined in solid vertical lines and various parts of the gradients are labeled below. Shown westerns are representative.

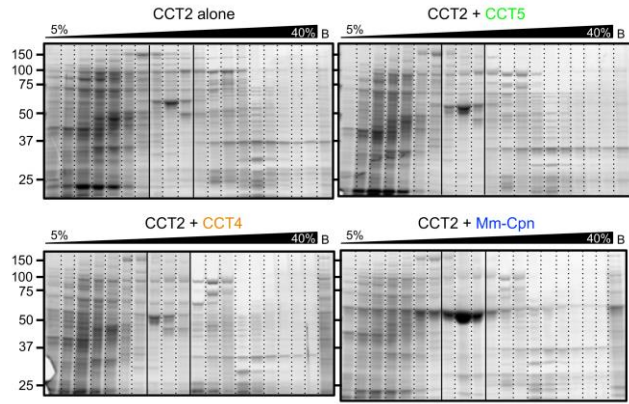
**Figure 3.** *Coexpression of homo-oligomerizing subunits with CCT1 does not change their position in the gradient.* Immunoblot SDS-PAGE of sucrose gradient ultracentrifugation performed as in Fig. 1. In *A*, CCT4, Mm-Cpn, and CCT5 sedimentation is shown when they are co-expressed with CCT1. In *B*, CCT4, Mm-Cpn, and CCT5 sedimentation is shown in other gradients where they are primarily expressed alone. For Mm-Cpn, there is no antibody available, but its expression is very high so its shadow can be seen on all western blots. Fractions are separated by dotted vertical lines for easier visual comparison, fractions corresponding to approximately the complex region of the gradient are outlined in vertical lines and various parts of the gradients are labeled below.

**Figure 4.** *A. CCT1 fast-sedimenting species associate with ribosomes.* CCT1 alone lysates were not treated (*top*) or treated (*bottom*) with EDTA and RNase to disrupt ribosomes. *B. Purification of CCT1 as eluted off of size exclusion chromatography.* CCT1 was purified as previously described for CCT4 and CCT5 homo-oligomers and the chromatography step was followed by coomassie staining (*top*) or antibodies against CCT1 (*bottom*). The fraction in red (11 mL elution from the size exclusion column) was chosen as the cleanest one to check by electron microscopy or mass spectrometry. *C. Electron microscopy of “purified” CCT1 shows ribosomes.* Negative-stain electron microscopy was performed on the fraction identified in B. Ribosomes (*circled*) and GroEL (*arrows*) are observed, suggesting ribosomes co-purify with CCT1. *D. Mass spectrometry of “purified” CCT1 is enriched in ribosomal proteins.* LC-MS/MS on the fraction identified in B shows mammalian CCT1 but also contaminating bacterial ribosomal proteins and chaperones.

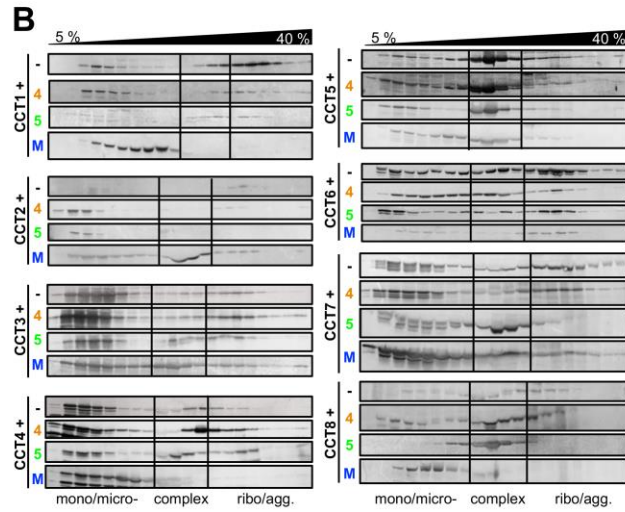
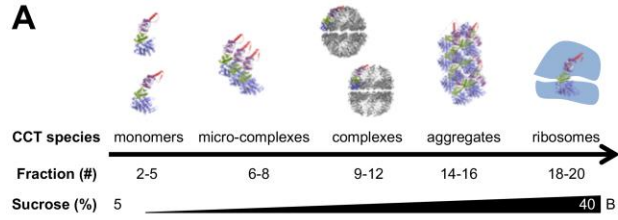
**Figure 5.** *A. Quantified densities of full-length CCT species for each set of sucrose ultracentrifugation gradients.* Full-length CCT species from Fig. 2 were quantified using ImageJ. The density in each fraction was divided by the total density of all fractions in a given gradient and is plotted here. Lines correspond to either each CCT subunit: alone, black; with CCT4, orange; with CCT5, green; or, with Mm-Cpn, blue. Solid vertical lines correspond to approximate complexes sedimenting in the gradient. Asterisks indicate areas where there was enrichment in species as compared to that CCT subunit alone, and are colored in agreement with the lines. The profiles of CCT subunit alone are shaded in grey for ease of viewing. *B. Binary heat map of CCT subunit complex formation alone, with CCT4, CCT5, or Mm-Cpn.* A heat map based on whether a complex species is present (black) for each CCT subunit in the data. Almost all CCT4 and CCT5 interactions are shown in grey and hashed because they form established complex species.

**Figure 6.** *A. Immunoblot SDS-PAGE of sucrose gradient ultracentrifugation of CCT1 alone or with Mm-Cpn. Performed as in Fig. 2; full-length CCT1 is indicated with solid arrows and various CCT1 fragments are labeled and indicated with dashed arrows. Fractions are separated by dotted vertical lines for easier visual comparison, fractions corresponding to approximately the complex region of the gradient are outlined in vertical lines and various parts of the gradients are labeled below. B. Quantified densities of fragmented CCT species for each set of sucrose ultracentrifugation gradients. Quantification were done and displayed as in Fig. 5. The fragments shown here are the only ones with significant changes. Other fragments that were analyzed but had no changes were: 36-kDa CCT2, 27-kDa CCT3, 35-kDa CCT4, 40-kDa CCT5, 35-kDa CCT7, and 35-kDa CCT8.*

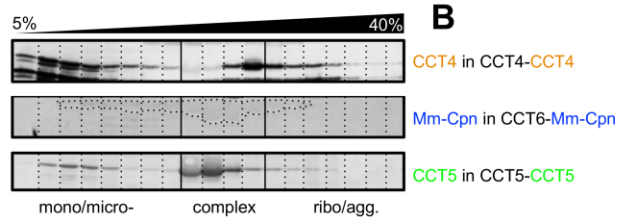
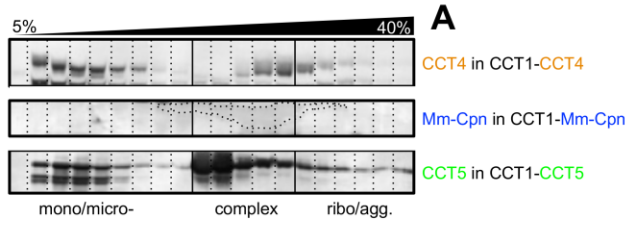
**Figure 7.** *A model of CCT subunit arrangement based on hetero-oligomerization data and the known CCT subunit order. Starting from CCT5 homo-oligomers, this theoretical model would show sequential subunit exchange to finally form the known CCT subunit order (Leitner et al. 2012). In the first step, CCT2 enters one ring [our data: CCT5 interacts with CCT2]. Since CCT2 forms intra-ring contacts, another CCT2 will enter the opposite ring [our data: CCT5 interacts with CCT2; final structure: CCT2 forms homo-typic contacts with itself while being adjacent to CCT5]. Next, CCT4 forms inter-ring contacts with CCT2 and CCT5 [our data: CCT5 interacts with CCT2 and CCT4; final structure: CCT4 is adjacent to CCT2]. Now, CCT1 can form inter-ring contacts with CCT4 [our data: CCT5 interacts with CCT1 and CCT2; final structure: CCT1 is adjacent to CCT4]. Subsequently, CCT3 forms inter-ring contacts with CCT4 while being adjacent to CCT1 and CCT1 forms intra-ring contacts with CCT7 [our data: CCT5 interacts with CCT2, CCT3, and CCT7; final structure: CCT3 is adjacent to CCT1, while CCT7 is on top of CCT1 while being adjacent to CCT5]. Next, CCT8 forms intra-ring contacts with CCT3 while being adjacent to CCT7 [our data: CCT5 interacts with CCT2, CCT3, CCT7, and CCT8; final structure: CCT8 is adjacent to CCT7 while being on top of CCT3]. Finally, CCT6 takes its place between CCT3 and CCT8 while making homo-typic contacts with itself [our data: CCT6 does not interact with CCT5 nor CCT4; final structure: CCT6 forms homo-typic contacts with itself while being adjacent to CCT3 and CCT8].*



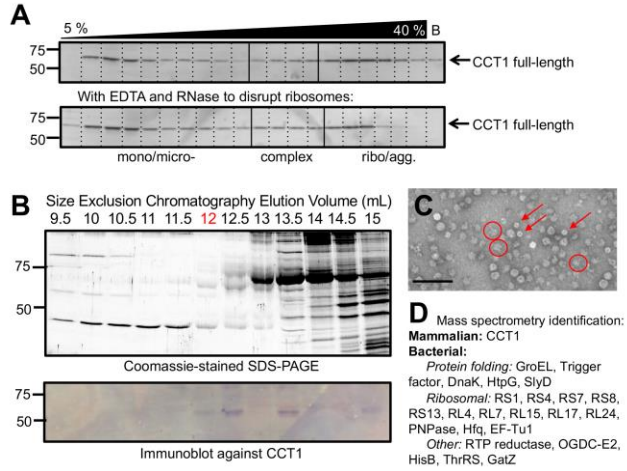
Author accepted manuscript



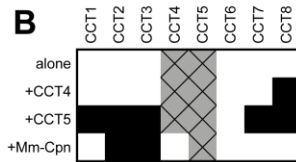
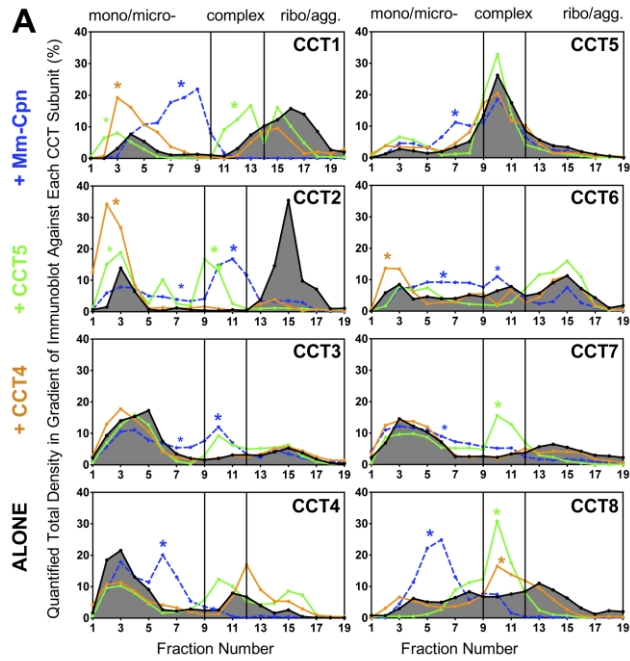
Author accepted manuscript



Author accepted manuscript

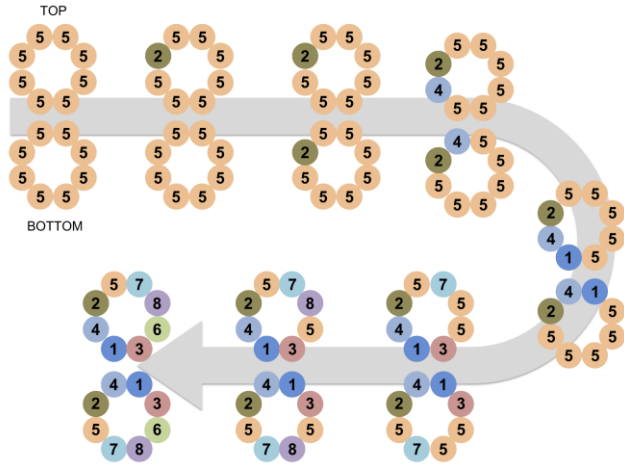


Author accepted manuscript









Author accepted manuscript